remote sensing

MDPI

Article

Bounding Surfaces in a Barchan Dune: Annual Cycles of Deposition? Seasonality or Erosion by Superimposed Bedforms?

Charles S. Bristow

Department of Earth and Planetary Sciences, Birkbeck, University of London, Malet Street, London WC1E 7HX, UK; c.bristow@ucl.ac.uk

Received: 11 March 2019; Accepted: 9 April 2019; Published: 23 April 2019

Abstract: A barchan dune near Tarfaya in Morocco has been surveyed using ground-penetrating radar (GPR) revealing packages of dipping strata within the dune that are truncated by bounding surfaces. The bounding surfaces dip in the downwind direction, truncate sets of cross-stratification, and are themselves downlapped by dipping strata. Models of aeolian strata suggest that the bounding surfaces could be reactivation surfaces, an erosion surface formed when a dune is reshaped by a change in wind. Alternatively, they could be superposition surfaces formed by smaller bedforms migration over the dune surface. These two hypotheses are tested using a combination of field and satellite observations. The average annual migration rate for the barchan dune derived from satellite images, gives an annual migration rate of 21.4 m·yr^{-1}. The number of reactivation surfaces imaged within the dune by GPR appears to scale with the annual migrating rate and dune turnover time suggesting that at this location, annual cycles in the wind regime are a potential control on dune stratigraphy with reactivation surfaces generated by changes in the wind direction, including wind reversals in the winter months. Alternatively, it is hypothesized that erosion in the lee of small superimposed bedforms as they pass the dune crest and approach the brink at the top of the slipface will create superposition surfaces. The migration rate of superimposed bedforms with a wavelength of 20 m has been measured at 2 m·day^{-1}. This suggests that small superimposed bedforms will arrive at the dune crest approximately every 10 days. Thus, bounding surface created by erosion in the lee of superimposed dunes will be very common. Given that the turnover time of the barchan dune is estimated at 4.3 years, the number of superposition surfaces produced by the faster bedforms could be more than 100. The number of bounding surface imaged by a GPR profile along the length of the dune appears to support the wind-driven reactivation hypothesis. However, a GPR profile across the dune images many small trough sets, instead of a single slipface, suggesting that superimposed dunes play an important role in the stratigraphy of a relatively simple barchan dune.

Keywords: dune migration; geomorphology; stratigraphy; ground-penetrating radar

1. Introduction

Barchan dunes are curved-crested, crescentic bedforms, with a single slipface and two horns that extend downwind. They are commonly found in desert areas where there is a limited sand supply and a unidirectional wind regime [1,2]. Field and laboratory studies of barchan dunes have demonstrated relationships between the width, height, and velocity of barchan dunes showing that smaller barchans migrate faster than larger barchans [3–9], and that large barchan dunes can support superimposed bedforms [10]. In addition, barchans have been observed to reverse and change shape in response to temporal changes in the wind regime [11]. Barchan dunes are said to be the simplest dune form, and their morphodynamics have been studied by engineers, geomorphologists, and physicists [3–9].

However, there have been relatively few studies of their internal structure. In an historic study, published in 1966, two trenches were cut through an 8.2 m high, 88 m wide, and 51 m long barchan dune at White Sands National Monument [12]. The strata recorded in that study will be compared with the radar images of the strata within the similar-sized barchan dune studied here.

Morphological changes in dunes are recorded by the sedimentary structures within the dunes. As dunes migrate downwind, layers of sand are deposited on the slipface on the lee-side of the dune. These steeply inclined layers of sand are termed cross-strata and record successive positions of the dune slipface. Sets of cross-strata are enclosed by bounding surfaces [13,14]. Kocurek [14] defined two common types of bounding surfaces within dune sands, reactivation surfaces and superposition surfaces. Reactivation surfaces are formed when a sand dune is reshaped by a change in the wind direction or wind velocity which reshapes a dune, eroding sand from one part and depositing it on another. In most parts of the world, the wind changes repeatedly with the passage of depressions or high-pressure cells and sand transport across dunes responds accordingly so that reactivation surfaces are very common if not ubiquitous. If the wind reverses, then the crest of the dune can be flipped, strata on the lee-side become truncated, and the stoss-side buried until the wind switches back again and the dune morphology is re-established [15]. If changes in the wind regime are regular or seasonal, then the reactivation surfaces may be cyclic, as has been observed in the Jurassic Navajo Sandstone in Utah [16]. These cycles might even be annual [17–19].

Superposition surfaces are formed where one dune migrates over another dune. This is most likely to occur where small fast-moving dunes migrate over larger slower-moving dunes or when small dunes are superimposed on the flanks of larger dunes, for example, where transverse dunes migrate across larger dune bedforms called megadunes. Within the rock record, it is difficult to distinguish between reactivation surfaces and superposition surfaces where both have similar orientations [14]. More recently, attention has turned to interactions between dunes as potential drivers of changes in dune morphology and erosion surfaces [20], although while dune interaction architecture has been identified in modern dune fields, it is yet to be widely applied to dune interpretation in the rock record [21].

Dune strata can be imaged by ground-penetrating radar (GPR) profiles [22–29]. In this paper, ground-penetrating radar (GPR) is used to image the internal structure of a barchan dune which includes sets of cross-strata and bounding surfaces. Hypothetical origins for the bounding surfaces include: 1) Erosion during seasonal changes in wind regime, and 2) erosion by superimposed bedforms. A combination of field observations and remote sensing are used in this paper to investigate these hypotheses and discuss how the bounding surfaces might have formed. Satellite images are used to monitor the migration of the barchan dune in Morocco. The results of the GPR survey are compared with remote sensing data and calculations of the dunes migration rate to investigate the relative importance of superimposed bedforms and seasonal wind changes on the dune stratigraphy.

Study Site

Barchan dunes in southern Morocco, close to the town of Tarfaya, have been studied previously [10,11,30]. The dunes form part of what has been described as the longest barchan field on Earth [30], extending around 300 km south from Tarfaya [6]. The morphology of barchan dunes in this area has been studied [6,11]. The wind blows sand, sourced from the Atlantic Ocean, towards the south-southwest; and the field of barchan dunes are actively migrating across a sand-covered bedrock surface of Pliocene marine sediments at an elevation around 23 m. On the interdune surface, there is sparse vegetation with small nebkha dunes, as well as some anthropogenic disturbance which includes vehicle tracks and excavations for aggregate.

In an earlier study, a total station was used to measure profiles across eight dunes in a systematic manner and extracted dune metrics including, height, volume, width, and length [6]. Reference [11] used a combination of marker posts, optical measurements of angles, and a digital inclinometer to measure the height and surface slopes of 11 barchans that were between 1 m and 10 m high. Their results

showed that the dunes respond to seasonal changes in wind direction [11]. In this area, there are regular trade winds throughout the year with a unimodal wind rose, with wind from slightly east of north, around 25° (Figure 1), with a resultant drift potential (RDP)/ DP around 0.9 [10]. This N-NE to S-SW 'Alizee' wind is dominant during the summer months (April to August), which is when the dunes are most active according to Reference [11], and this is the period when the barchans travel the major part of their distance [11]. However, even in an area such as the Moroccan Atlantic Sahara, described as having some of the most stable wind conditions on Earth [11], barchan dunes have been observed to reverse and change shape in response to temporal changes in the wind regime (Figure 2a). As a consequence, barchan migration is far from constant over the year. Reference [11] indicates gradual changes in the rate of migration downwind, but more extreme changes were observed in the E–W orientation, across the dominant migration direction. Observations of barchan dunes in the field in January 2011 show reversed dune crests. This change in dune morphology is consistent with the wind data.

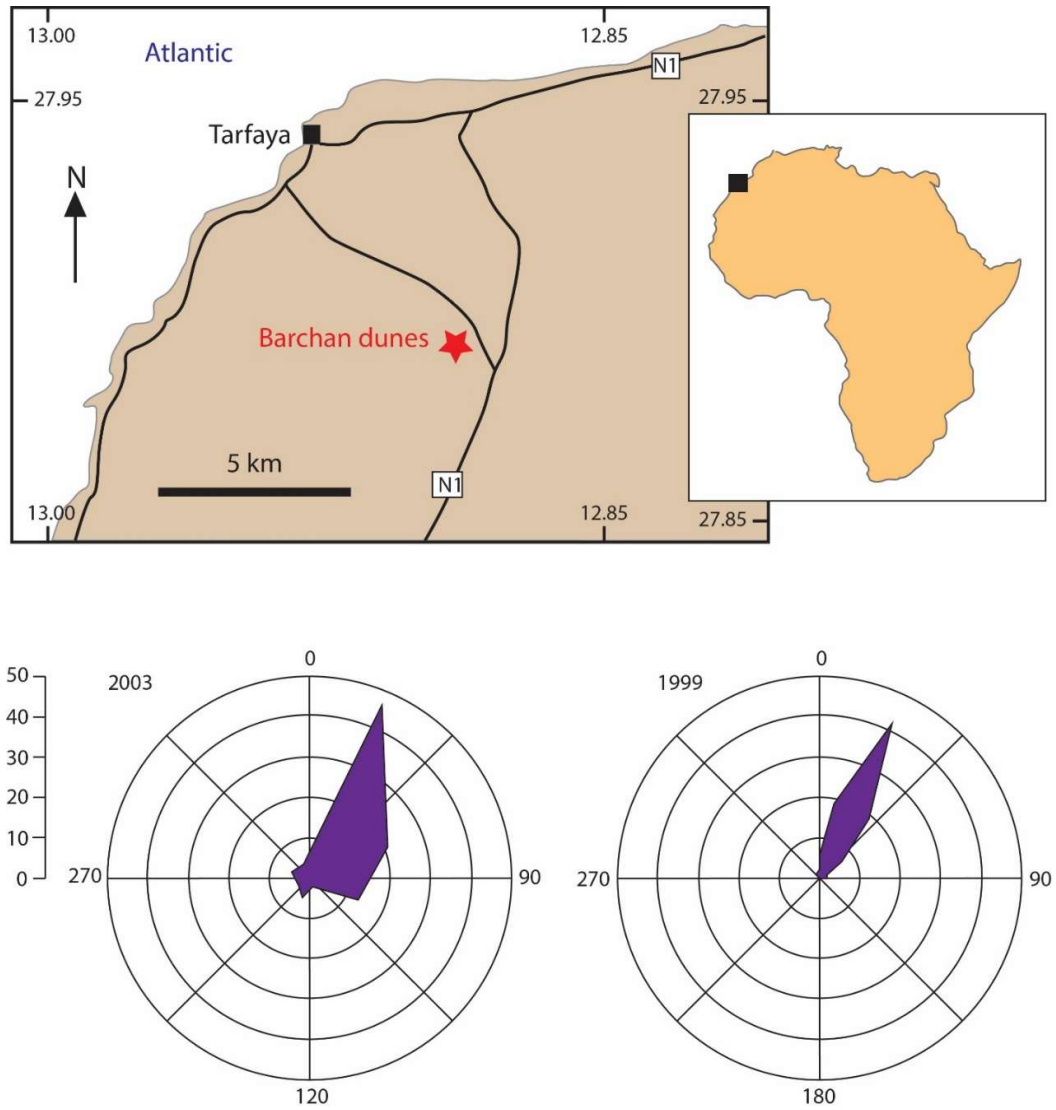

Figure 1. Location map for Tarfaya in southern Morocco showing the barchan dune described in this paper as well as wind roses for Tarfaya for 1999 and 2003, from El belrhiti and Douady 2011, the radial scale is the percentage of time.

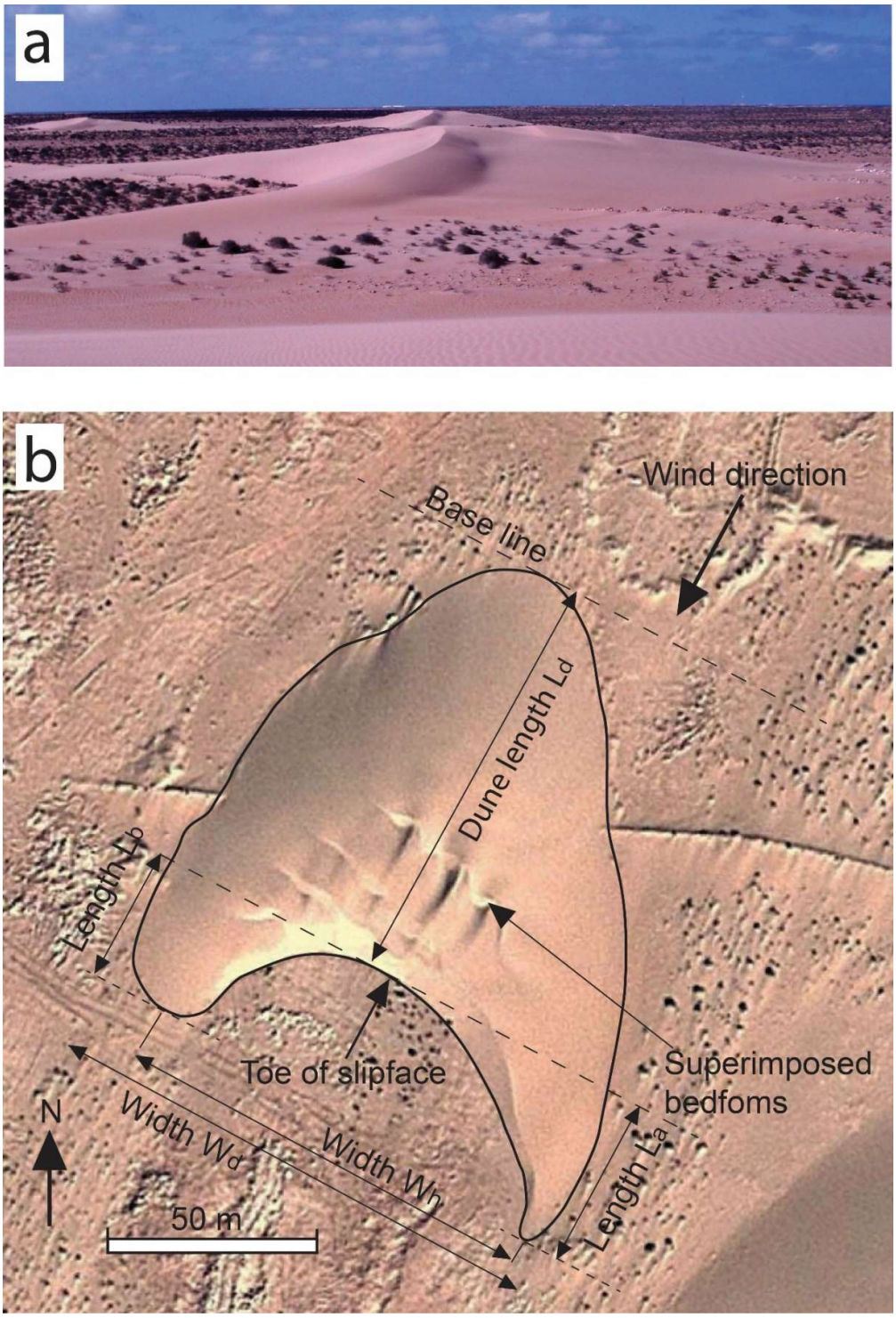

Figure 2. (**a**) Field photograph of barchan dunes near Tarfaya, taken by the author in January 2011; at that time, the wind had reversed, causing changes in the dune crest similar to those described by El belrhiti and Douady (2011). (**b**) Annotated satellite image of the studied barchan dune, image date December 15, 2012 Google Earth™ Pro, showing superimposed dunes developed on top of the barchan. The dimensions measured from satellite images following Finkel (1959) include: Length of the dune (Ld); the length of the horns (La and Lb); the width between the points of the horns (Wh); as well as the width of the dune at its widest point (Wd).

In addition to seasonal changes in morphology, the dunes support smaller bedforms on the windward (stoss slope) that have been described [5,11] (Figure 2b). The superimposed wave-like bedforms described by Reference [5] typically have wavelengths around 20 m, although longer wavelengths (λ = 28 m) were recorded on a megabarchan, and shorter wavelength (λ = 12.5) were measured on the horns of a barchan [5]. When these waves reach a sufficiently high amplitude, they develop a slipface [5,30]. Recirculating flow in the lee of a dune slipcase can create scour in the lee of the bedform, and the small superimposed dune can erode into the crest of the underlying dune (Figure 3).

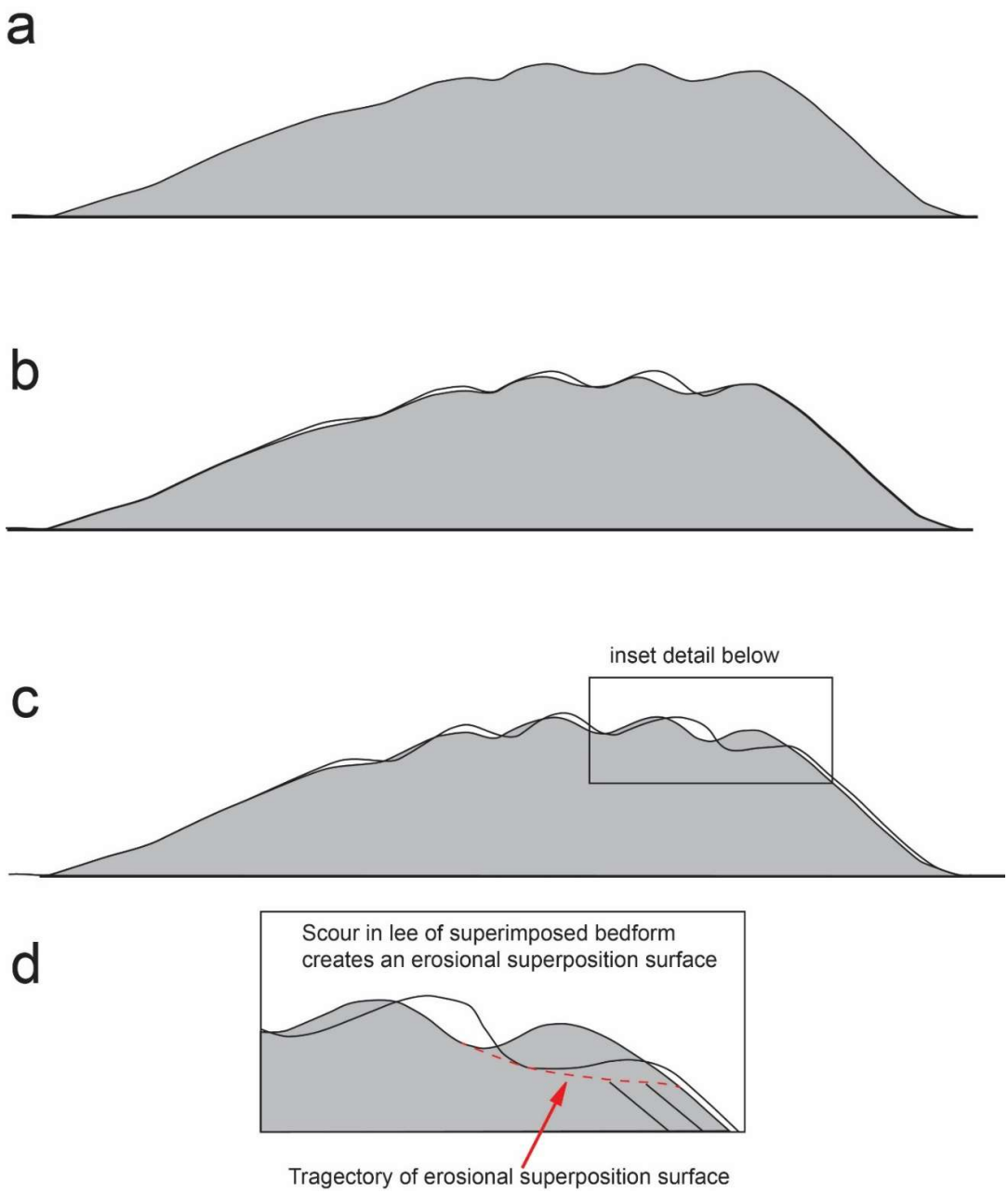

Figure 3. (**a**) Barchan dune with superimposed wave-like bedforms; (**b**) superimposed bedforms migrate faster than the barchan dune and increase in amplitude until they develop a slipface becoming a superimposed dune [30]; (**c**) scour in the lee of the superimposed dune erodes into the crest of the dune forming an erosional superposition surface; (**d**) inset detail showing trajectory of erosional bounding surface.

2. Methods

Satellite images in Google Earth™ Pro have been used to track the movement of a barchan dune between 2005 and 2018 (Figure 4). The outline of the dune was defined using the polygon tool in Google Earth™ Pro along the interface between the dune sand and the interdune. The contrast between the dune sand and the interdune areas varies between images. In general, the dune sand is a uniform pale brown while the interdune surface appears slightly darker on the satellite images. The interdune areas also shows vehicle tracks and dark dots of vegetation that are absent from the dune sands. In the earliest image dated May 11th, 2005, the edge of the dunes is locally picked out by a row of vegetation along the base of the dune. At other times this feature is absent. Determining the downwind termination of the horns of the barchan is a bit subjective because sand leaks from the horns, as noted by Reference [31], and spreads from the dune into the interdune area. However, the downwind margin of the dune at the slipface is usually sharply defined, and it is the position of the base of the slipface that has been used to calculate the dune movement. Picking independent ground control points to assess the accuracy of the measurements indicates image registration within Google Earth™ is ± 2 m, which is around 2% of the length and width of the dune.

The morphology of barchan dunes in Peru was described by Reference [4] and most of the parameters used by Reference [4] can be derived from satellite images, including the length of the dune (Ld), the length of the horns (La and Lb), as well as the width between the points of the horns (Wh) (Figure 2b). In addition, the width of the dune at its widest point (Wd) is measured because that is used in calculations of dune volume by other authors. In the field, the length and slopes of the dune were measured using tape measures and an inclinometer. The end points of the GPR profiles were located using a handheld GPS.

The ground-penetrating radar (GPR) data were collected using a Pulse Ekko 100 GPR with 100 and 200 MHz antennas. The antennas were placed on the ground in the parallel broadside configuration with 0.5 m separation for the 200 MHz antennas and 1.0 m separation for the 100 MHz antennas. Measurements were spaced at 0.5 m for the 100 MHz antennas and 0.2 m for the 200 MHz antennas. Two GPR profiles across the dune were collected with both antennas, one along the length of the dune from the downwind margin, over the crest of the dune, and down the slipface, and a second profile across the dune upwind from the brink. The GPR data have undergone minimal processing to preserve the integrity of the data [32,33], using only de-wow, AGC gain, and topographic correction. The velocity used for the topographic correction is 0.17 m ns^{-1}, which is within the range of velocities quoted for dry sands [34] and restores the base of the dune to the horizontal (Figures 5–7). Using a velocity of 0.17 m ns^{-1} with 200 MHz antennas gives a wavelength of 0.85 m and resolution of 0.21 at $\frac{1}{4}$ wavelength. For the 100 MHz antennas, the wavelength and resolution are around 1.7 m and 0.425 m, respectively.

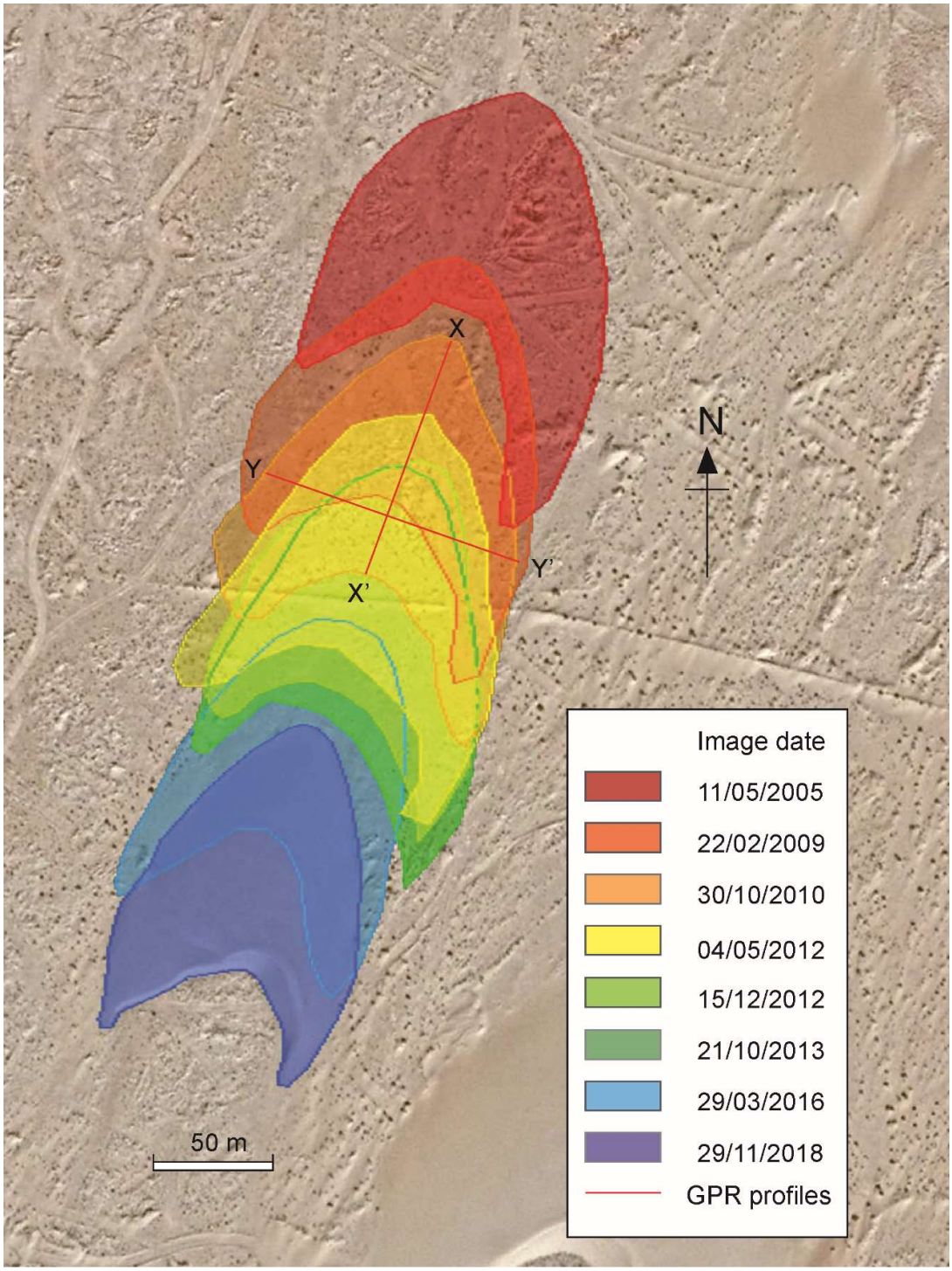

Figure 4. Outlines of the barchan dune near Tarfaya between 2005 and 2018, tracked using satellite images in Google Earth™ Pro. The dune has moved 290 m during this period of 13.5 years. The direction of migration has remained consistent over this period. The dark spots on the interdune surface are small shrubs that locally form nebkha dunes. Vehicle tracks also cross the interdune areas but do not appear to have influenced the dune movement.

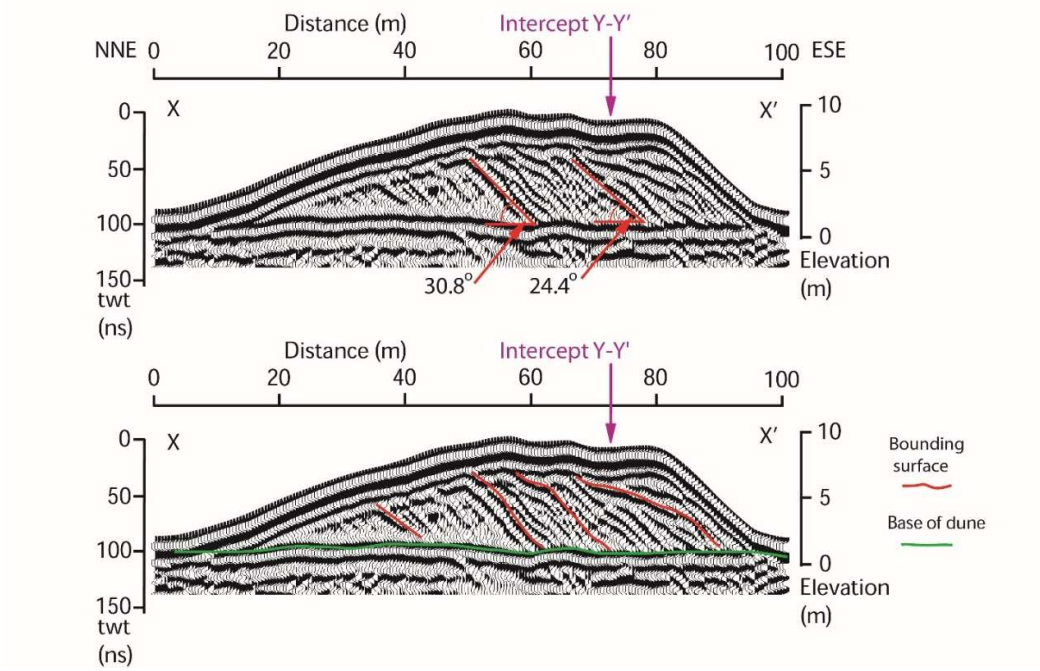

Figure 5. Ground-penetrating radar (GPR) profile along the length of the dune Y-Y′ (NNE-SSW) collected with 100 MHz antennas in January 2011. Continuous lines at the top of the dune are the direct signals between the transmitter and the receiver, first through the air (airwave) and second through the ground (groundwave). The inclined reflections within the dune record the former position of the slipface at the downwind side of the dune and are interpreted as cross-strata and bounding surfaces. Four bounding surfaces are picked in red where cross-strata are truncated. The continuous sub-horizontal reflections at the base of the dune come from the interdune surface (green line), modified from Reference [36].

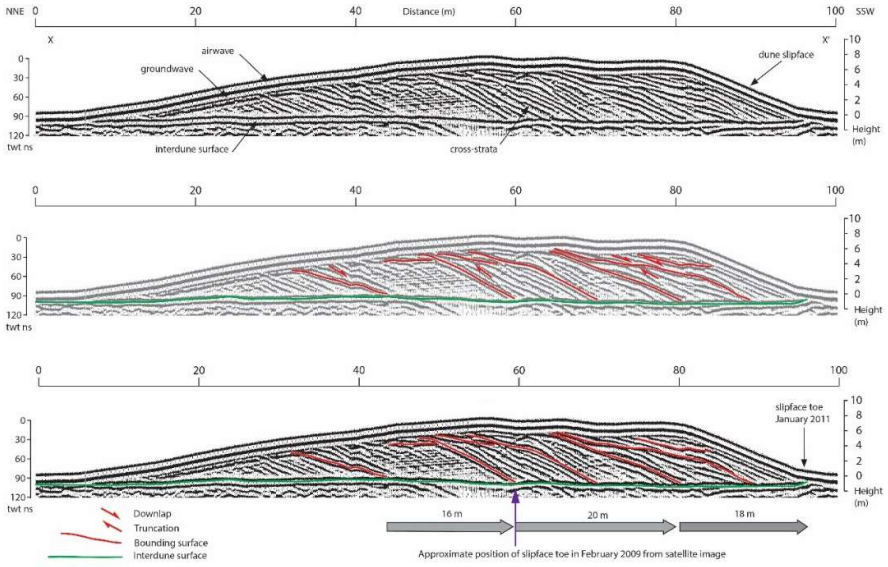

Figure 6. GPR profile along the length of the dune X-X′ (NNE-SSW) collected with 200 MHz antennas shows inclined reflections dipping in the downwind direction that are interpreted as cross-strata and bounding surfaces. Bounding surfaces are picked in red where cross-strata are truncated. The higher resolution obtained with 200 MHz antennas record more detail of the strata within the dune. Annual cycles are apparent, and the approximate position of the slipface toe in February 2009 is indicated. However, the higher resolution reveals additional bounding surfaces.

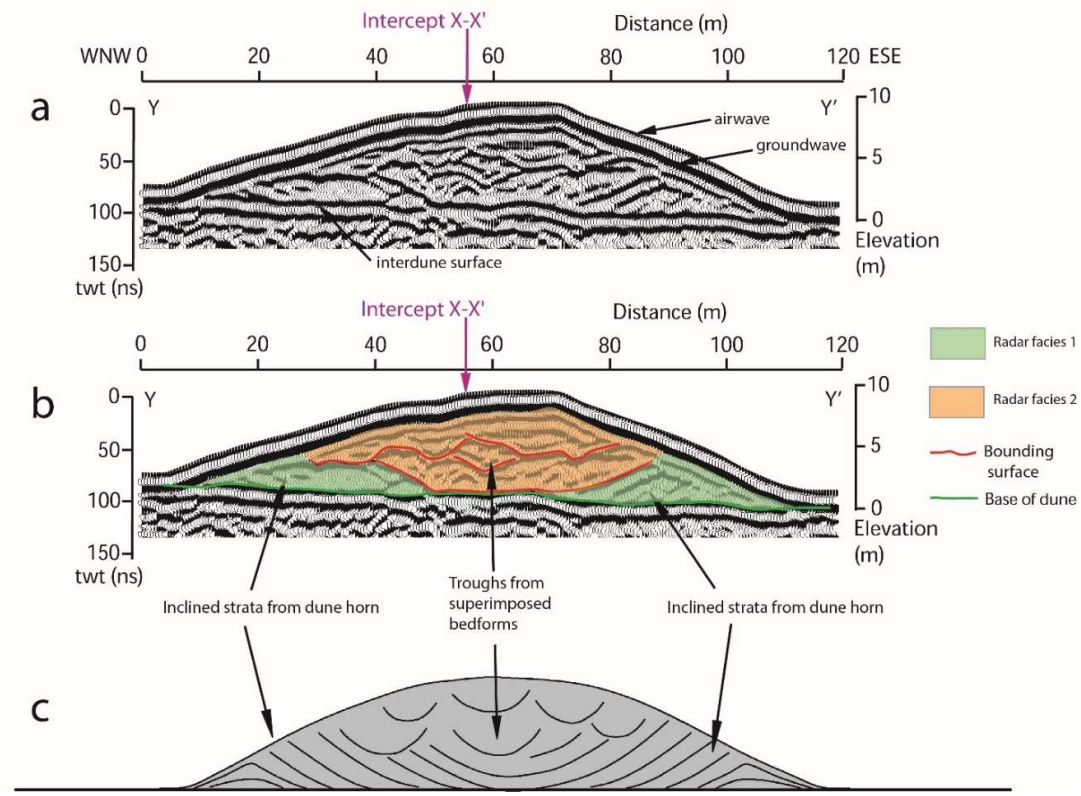

Figure 7. Ground-penetrating radar profile across the dune W-E collected with 100 MHz antennas in January 2011 (modified from Reference [35]); **a**) processed GPR data; **b**) interpretation of GPR profile; **c**) schematic sketch of dune cross-section. In a, continuous lines at the top of the dune are the direct signals between the transmitter and the receiver, first through the air (airwave) and second through the ground (groundwave). Planer-inclined reflections (RF1) within the lower part of the dune and at its margins are interpreted to be the deposits of the horns of the dune. Discontinuous concave reflections (RF2) within the middle and upper part of the dune are interpreted as sets of trough cross-strata likely to have been formed by superimposed dunes.

3. Results

At the time of the GPR survey in January 2011, the dune was around 98 m long and 7.8 m high. The dimensions of the dune have been measured eight times from satellite images between 2005 and 2018 (Table 1). The length, width, and asymmetry all vary from year to year although the variation is limited, and the dune morphology is relatively conservative. A reduction in the width of the dune indicates that it is getting narrower over time (Table 1). One of the notable features is that the asymmetry of the dune changes; between 2005 and 2016 the eastern horn is longer but in December 2018 it is the western horn that is longer. In a study of dune asymmetry, Reference [35] states, that barchan dune asymmetry can result from an asymmetric sediment influx, topography, collisions, and an asymmetric wind regime. In this case, a topographic effect, where dunes migrate across a sloping surface, can be ruled out because the plateau across which the dunes migrate is relatively flat. The studied dune does have a neighboring dune but it is not in collision with any other dunes, and there are no dunes immediately upwind that could cause an asymmetric sediment influx. It appears, therefore, that the asymmetry of the dune is a function of the wind regime. A change in the wind also helps to explain how the asymmetry of the dune can switch from a longer eastern horn to a longer western horn. Such a change is consistent with the lateral dune movements noted by Reference [11] and would be difficult to explain otherwise.

Table 1. Dune dimensions extracted from satellite images using Google Earth™ pro.

Date	Width Wd (m)	Width Wh (m)	Length Ld (m)	East Horn La (m)	West Horn Lb (m)	La/Lb
11/05/2005	122	103	94	78	43	1.8
25/02/2009	127	104	104	63	33	1.9
30/10/2010	129	110	104	57	36	1.6
04/05/2012	126	106	104	59	37	1.6
15/12/2012	116	97.5	103	49	26	1.9
21/10/2013	117	103	108	60	33	1.8
29/03/2016	106	98.7	94	56	46	1.2
29/11/2018	103	79	105	39	42	0.9
Mean	118.25	100.15	102	57.6	37	
Standard deviation	9.7	9.4	5.2	11.2	6.5	

3.1. Dune Migration

During the period of 13.5 years between May 2005 and December 2018, the dune has migrated 290 m downwind, an average of 21.4 m·yr^{-1}, while the dune on the right, which is slightly larger, has an average migration rate of 16.4 m·yr^{-1}. Between successive images, the migration rates range from 23.6 to 14.3 m·yr^{-1} (Table 2). These figures for dune velocity are close to the velocities for similar-sized dunes near Tarfaya [31], and slightly lower than the velocity of dunes to the south near Laayoune [31].

Table 2. Rates of dune migration at Tarfaya derived the locations of the dune slipface toe from satellite images using Google Earth Pro™.

Image Date from	Image Date to	Time Difference (years)	Distance Moved (m)	Annual Migration Rate (m/yr)
11/05/2005	25/02/2009	3.6	85	23.6
25/02/2009	30/10/2010	1.68	32	19
30/10/2010	04/05/2012	1.58	33	20.1
04/05/2012	15/12/2012	0.88	13	22.4
15/12/2012	21/10/2013	0.84	12	14.3
21/10/2013	29/03/2016	2.4	53	22
29/03/2016	29/11/2018	2.7	58	21.5
11/05/2005	29/11/2018	13.55	290	21.4

3.2. GPR Profiles

At the top of the GPR profiles are a pair of black and white (positive and negative) signals that are the airwave and the groundwave (Figures 5–7). The airwave is the direct arrival from the transmitter to the receiver through the air at the speed of light. The groundwave is the direct arrival from the transmitter to the receiver through the ground, which travels at a lower velocity determined by the dielectric properties of the dune sand. Beneath the airwave and the groundwave are reflections that come from changes in the sand layers within the dune, and the interdune surface at the base of the dune. Reflections can come from changes in the grain size of the sand, compaction, or moisture content [22,26,27]. These layers record the position and shape of the lee-side of the dune, and have been buried and preserved within the dune as it migrates downwind. At the base of the dune, there is a continuous high-amplitude reflection from the interdune surface that is visible on all of the GPR profiles.

4. Discussion

The migration rates of barchan dunes have been documented to show an inverse relationship between dune height and celerity [37]. Using Google Earth™ Pro, it has been possible to track the movement of the barchan that was surveyed in 2011 and calculate an average migration rate for the dune. Between May 2005 and the end of December 2018, the dune moved 290 m, giving an annual rate of migration of 21.4 m·yr^{-1}. During the same period, the next dune to the east, which is a slightly larger dune, moved 226 m, giving an annual migration rate of 16.7 m·yr^{-1}. These rates of migration are within the range of migration rates compiled from other studies of barchan dunes of similar height that range between 7 m·yr^{-1} to over 34 m·yr^{-1} [37].

4.1. Sand Flux

Following Reference [7] and Reference [9], Q_{dunes} is defined as the dune's mass of sand transported through a width W at a speed C. The average value once a dune has migrated over a distance equivalent to its length along the transport direction is given by Equation (1). Assuming that barchan dunes have a scale-independent shape, the volume of the dune can be estimated using a scaling law $V = k*W^3$ (Duran et al., 2010). However, the constant k appears to be different for barchan dunes from different parts of the world. For their simulated barchan dunes, Reference [8] obtained a value of 0.017, while Reference [9] derived a value of 0.00833 based on the volume of a single barchan dune in Qatar. For this study, we used the dune width and dune volume data from Reference [6] who surveyed eight barchan dunes in southern Morocco. A cross-plot of dune volume against W^3 gives a value for k of 0.032. It should be noted that the measurement of W is important because W is cubed. Reference [6] used the width between the dune horns (Wh), while Reference [9] appear to use the width of the widest part of the dune (Wd).

$$\text{Equation 1. } Q_{dunes} = (1-\phi)\rho s\, VC/WL \quad (1)$$

where V is the volume of the dune in m^3, C is the dune velocity in m·yr^{-1}, W is the dune width in m, L is the mean dune length, ρs is the volumetric mass density, and ϕ is the porosity of the dune. Using the width between the dune horns (Wd), the sand flux is estimated at 77,414 kg m^{-1} yr^{-1}.

4.2. Dune Turnover Time and Superimposed Bedforms

Given that the length of the dune from the upwind end to the base of the slip face is 98 m, and an average annual rate of migration of 21.4 m·yr^{-1}, the turnover time for the dune should be 4.6 years. This means that the dune should preserve a record of around four and a half years of deposition. While the annual rate of dune migration varies between 14.3 and 23.6 m·yr^{-1} (Table 2), it is typically ~21 m·yr^{-1}. The rate of migration of the smaller wave-like undulations superimposed on the dune surface propagate downwind at a rate of 2 m/day [10], which would be over 700 m·yr^{-1}. At this rate, it would take a superimposed bedform around 40 days to migrate up the stoss-side of the dune, with a

superimposed bedform arriving at the dune crest every 10 days. Extrapolating this over the turnover time of the barchan dune, which is 4.6 years or 1671 days, then as many as 150 superimposed bedforms might arrive at the dune crest during a single dune turnover. These calculations make some gross assumptions about the amount of time that the dune is active and ignore the periods when the winds are reversed. However, even if superimposed bedforms are only generated for six months of the year, when the dunes are most active, there would be time for many tens of superimposed bedforms to arrive at the dune crest. Furthermore, the superimposed bedforms on the dune studied have a wavelength of around 10 m and are likely to migrate faster than the 20 m bedforms described by Reference [10].

4.3. Discussion of GPR Interpretation

The 100 MHz profile along the length of the dune X-X′ shows the pair of black and white reflections from the airwave and the groundwave at the top as well as the continuous high-amplitude reflection from the interdune surface at the base of the dune (Figures 5–7). The 100 MHz GPR profile along the length of the dune shows inclined reflections interpreted as cross-strata and bounding surfaces (Figure 5). The cross-strata have dips of 30.8° and 24.4°, which are steeper than the dips of the bounding surfaces (Figure 5). The number of bounding surfaces picked (four) is consistent with the dune turnover time (4.6 years). However, the distance between the bounding surfaces is less than the average annual dune migration rate. In addition, the spacing of the bounding surfaces is irregular (Figure 5), while the annual dune migration rates appear to be reasonably consistent (Table 2 and Reference [11]). This observation does not rule out the possibility of annual cycles, but does suggest that there are other effects at play.

On the 200 MHz GPR profile along the length of the dune X-X′ (Figure 6), the steeply dipping, planar-inclined reflections within the dune are interpreted as sets of cross-strata. The lower-angle reflections are interpreted as bounding surfaces within the dune (Figure 6). Erosional bounding surfaces are picked where they truncate underlying reflections and also where they are downlapped by overlying reflections (Figure 6). The truncation of reflections marks a period of erosion, either due to reshaping of the dune by wind erosion or erosion in the lee of a superimposed bedform. The 200 MHz data have a higher resolution and record more detail of the dune strata and images a greater number of bounding surfaces than the 100 MHz data. Using the satellite imagery to reconstruct the position of the toe of the dune slipface in 2009 appears to confirm the presence of a winter reactivation surface. However, additional bounding surfaces are revealed, and it is obvious that these cannot all be attributed to an annual cycle given the location and migration of the dune recorded from satellite images. It is not possible from the profile along the dune alone to determine the cause of these erosion surfaces.

The GPR profile across the dune Y-Y′ (Figure 7) shows the airwave and the groundwave along the dune surface as well as the high-amplitude reflection from the interdune surface at the base of the dune. Within the dune, two types of reflection pattern, or radar facies, are identified. Radar facies 1 (RF1) are planar-inclined reflections. Radar facies 2 (RF2) are discontinuous concave reflections. The planar-inclined reflections (RF1) are found towards the base of the dune and at its margins (Figure 7). The reflections on the east side of the dune dip towards the west, while the reflections on the west side of the dune are lower-angle, less well resolved, and dip towards the east. The planar-inclined reflections (RF1) are interpreted to have been formed on the inside of the horns of the dune where they merge with the slipface. They show convergent dips due to the curvature of the slipface and are preserved at the base of the dunes because the width of the dune horns (Wh) is less than the width of the dune (Wd), so that the dune overrides its horns. The westward-dipping cross-strata is larger because the eastern horn of the dune was dominant at the time of the GPR survey in 2011. The discontinuous concave reflections (RF2) are located in the middle of the dune and are interpreted to be sets of trough cross-strata. The presence of many troughs rather than a single large set is interpreted to be the effect of superimposed dunes (Figure 7c).

4.4. Comparison with the Trench Sections Cut by McKee 1966

The results of the GPR survey are compared with trench sections excavated through a barchan dune [12]. The dune trenched by Reference [12] was a similar height to the barchan studied here, a little narrower (Wh = 88.4 m instead of 100.15 m), but shorter (51.8m against 102 m), and less well defined. Sketch maps in Reference [12] indicate a barchanoid form connected to other dunes rather than a true barchan that is isolated from other dunes. The section parallel to the direction of dune migration was dominated by tabular planar cross-strata dipping at 26° to 34° in the downwind direction. Bounding surfaces in the upwind half of the dune were low-angle dipping at 2°–6° in the downwind direction and steepening to 20°–28° towards the downwind end of the dune [12]. There are some similarities to the strata imaged in the GPR profiles with cross-strata dipping downwind at similar angles (Figure 5), and bounding surfaces dipping downwind, but the dune excavated by Reference [12] contained many more bounding surfaces.

In the section cut perpendicular to the dune, migration direction that cut through one half of the dune revealed sets of cross-strata 0.6 to 1.5 m thick that tapered towards the dune margins with near-horizontal bounding surfaces [12]. The cross-strata had apparent dips of around 20° and dipped towards the outside of the dune. This description contrasts with the transverse section through the barchan dune described in this paper. In the section through a dune horn described by Reference [12], strata dip towards the outside of the dune, whereas in this study the GPR reflections indicate strata dipping towards the inside of the dune. The difference is attributed to a greater curvature of the dune slipface in Morocco, and the width across the dune horns vs. the dune width. In Morocco, the width across the dune horns (Wh) is less than the width of the dune (Wd), which results in the dune riding over the horns and preserving their deposits. In addition, discontinuous concave reflections, interpreted as sets of trough cross-strata, fill the central and upper part of the dune in Morocco. At White Sands, trough structures were observed but these were interpreted as blowout structures and were described as forming 'only a very minor part of the total structure' [12] p. 40. The asymmetric troughs interpreted as blowouts by Reference [12] might now be interpreted as superimposed dunes. In addition, the near-horizontal bounding surfaces within the White Sand's dune might now be interpreted as superposition surfaces, produced by smaller superimposed bedforms.

Some of the differences in sedimentary architecture between the White Sands barchan and the Morocco barchan can be attributed to differences in dune morphology because the White Sands barchan trenched by Reference [12] was barchanoid rather than a true barchan. Few dunes have the idealized form and most have some perturbation. The sedimentary structures within dunes provide a record of morphological changes such as bounding surfaces produced by reversing winds (Figure 8). These structures can be imaged by ground penetrating radar profiles obviating the requirement for trenching. However, a three-dimensional view is required to check real and apparent dips and reconstruct the dune architecture. In this study, a relatively simple barchan in an area that is supposed to have some of the most stable wind conditions on Earth [10,31] shows a complex internal structure because the fluctuation of the wind is sufficient to perturb the shape of the dune, reshaping the dune during reversing winds and oblique winds. In addition, the development of superimposed bedforms appears to have had a significant impact on dune strata with multiple troughs recorded in place of a single slipface.

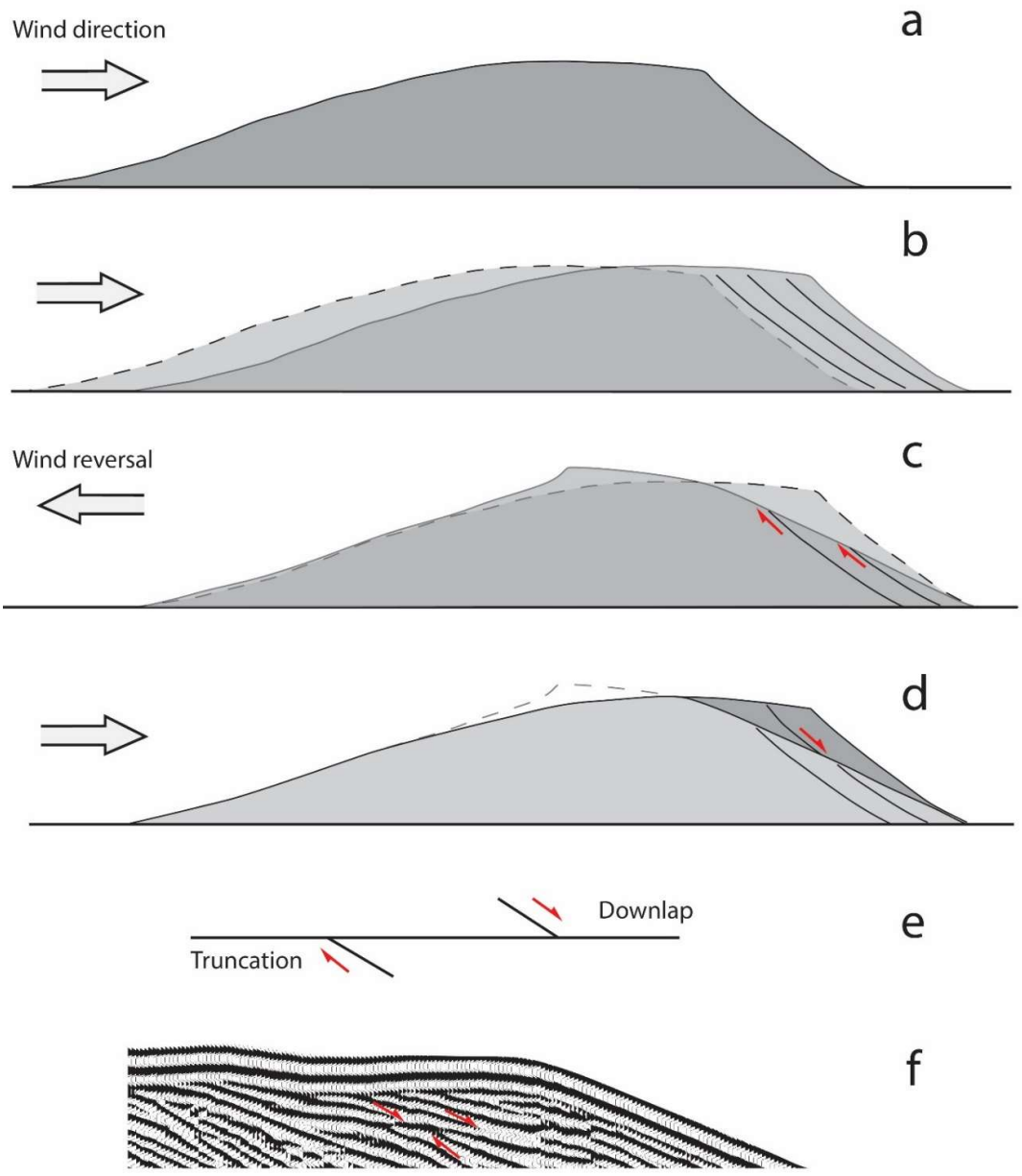

Figure 8. Formation of reactivation surfaces following a reversal in the wind direction; (**a**) section through a barchan dune with wind from left to right; (**b**) dune migrates downwind preserving cross-strata that record the former position of the lee-side slipface; (**c**) wind reversal. Wind blowing from right to left reshapes the dune, erodes sand from the slipface and the brink of the dune, and deposits sand on the dune crest with a smaller, reversed slipface. Erosion of the slipface truncates existing cross-strata; (**d**) wind direction switch back to left to right. The dune slipface is reformed with cross-strata downlapping onto the erosion surface forming a reactivation surface; (**e**) illustration of truncation and downlap; (**f**) examples of truncation and downlap as they appear on the GPR profile.

5. Conclusions

Dune tracking using freely available satellite images can be used to estimate rates of dune migration and monitor changes in sand dune morphology. The results of this study show a relatively consistent annual rate of dune migration of 21.4 m·yr^{-1} over a period of 13.5 years (2005–2018), and a dune turnover time of 4.6 years.

GPR profiles along the length of the dune show dipping reflections interpreted as sets of cross-strata. Lower-angle bounding surfaces truncate underlying inclined strata and are, in turn, down-lapped by

overlying sets of cross-strata. These bounding surfaces could be superposition surfaces, formed by erosion in the lee of smaller superimposed bedforms, or reactivation surfaces formed by reshaping of the dune by changes in the wind direction. As noted by Reference [14], it can be very difficult to distinguish between superposition surfaces and reactivation surfaces in sections parallel to the dune migration direction.

The number of bounding surfaces visible on a 100 MHz GPR profile along the length of the dune is consistent with the measured annual rates of dune migration and the calculated turnover time, although the spacing is quite variable. These observations could support the hypothesis that seasonal changes in the wind regime forming reactivation surfaces in the barchan dunes at Tarfaya. However, a higher frequency (200 MHz) GPR profile with improved resolution shows a greater number of bounding surfaces. Furthermore, a GPR profile across the dune reveals converging strata at the base of the dune overlain by several small trough sets rather than a single large trough from the slipface. The convergent strata are interpreted to be formed by the dune horns. The multiple small troughs are interpreted to be formed by small superimposed dunes which generate superposition surfaces. Thus, the cross-section view, perpendicular to the dune migration, suggests that the bounding surfaces are likely to be superposition surfaces generated by small superimposed bedforms.

It is most likely that both types of bounding surface are present within the dune; reactivation surfaces caused by changes in the wind direction including wind reversals, as well as superposition surfaces formed by superimposed bedforms. The results support the comments in Reference [14] regarding the identification of different types of bounding surface in the downwind direction and demonstrate that a 3-D view is required to make meaningful reconstructions of dune strata.

Funding: This research received no external funding.

Conflicts of Interest: The authors declare no conflict of interest.

References

1. McKee, E.D. *A Study of Global Sand Seas*; Geological Survey Professional Paper 1052; United States Government Printing Office: Washington, DC, USA, 1979; 429p.
2. Wasson, R.J.; Hyde, R. Factors determining desert dune type. *Nature* **1983**, *304*, 337–339. [CrossRef]
3. Bagnold, R.A. *The Physics of Blown Sand and Desert Dunes*; Methuen & Co. LTD.: London, UK, 1941; 265p.
4. Finkel, H.J. The Barchans of southern Peru. *J. Geol.* **1959**, *67*, 614–647. [CrossRef]
5. Long, J.T.; Sharp, R.P. Barchan-dune movement in imperial valley, California. *Geol. Soc. Am. Bull.* **1964**, *75*, 149–156. [CrossRef]
6. Sauermann, G.; Rognon, P.; Poliakov, A.; Herrmann, H.J. The shape of the barchan dunes of Southern Morocco. *Geomorphology* **2000**, *36*, 47–62. [CrossRef]
7. Ould Ahmedou, D.; Ould Mahfoudh, A.; Dupont, P.; Ould El Moctar, A.; Valance, A.; Rasmussen, K.R. Barchan dune mobility in Mauritania related to dune and interdune sand fluxes. *J. Geophys. Res.* **2007**, *112*, F02016. [CrossRef]
8. Duran, O.; Parteli, E.J.R.; Herrmann, H.J. A continuous model for sand dunes: Review, new developments and application to barchan dune fields. *Earth Surf. Process. Landf.* **2010**, *35*, 1591–1600. [CrossRef]
9. Michel, S.; Avouac, J.-P.; Ayoub, F.; Ewing, R.; Vriend, N.; Heggy, E. Comparing dune migration measured from remote sensing with sand flux prediction based on weather data and model, a test case in Qatar. *Earth Planet. Sci. Lett.* **2018**, *497*, 12–21. [CrossRef]
10. Elbelrhiti, H.; Claudin, P.; Andreotti, B. Field evidence for surface-wave—Induced instability of sand dunes. *Nature* **2005**, *437*, 720–723. [CrossRef]
11. El belrhiti, H.; Douady, S. Equilibrium versus disequilibrium of barchan dunes. *Geomorphology* **2011**, *125*, 558–568. [CrossRef]
12. McKee, E.D. Structures of dunes at White Sands National Monument, New Mexico (and a comparison with structures of dunes from other selected areas). *Sedimentology* **1966**, *7*, 3–69. [CrossRef]
13. Brookfield, M.E. The origin of bounding surfaces in ancient aeolian sandstones. *Sedimentology* **1977**, *24*, 303–332. [CrossRef]

14. Kocurek, G.A. Desert aeolian systems. In *Sedimentary Environments: Processes, Facies and Stratigraphy*; Reading, H.G., Ed.; Blackwell Science: Hoboken, NJ, USA, 1996; pp. 125–153.
15. Bristow, C.S.; Augustinus, P.C.; Wallis, I.C.; Jol, H.M.; Rhodes, E.J. Investigation of the age and migration of reversing dunes in Antarctica using GPR and OSL, with implications for GPR on Mars. *Earth Planet. Sci. Lett.* **2010**, *289*, 30–42. [CrossRef]
16. Loope, D.B. Episodic deposition and preservation of eolian sands—A late Paleozoic example from southeastern Utah. *Geology* **1985**, *13*, 73–76. [CrossRef]
17. Chan, M.A.; Archer, A.W. Spectral analysis of eolian foreset periodicities: Implications for Jurassic decadal-scale paleoclimatic oscillators. *Paleoclimates* **1999**, *3*, 239–255.
18. Loope, D.B.; Rowe, C.M.; Joeckel, R.M. Annual monsoon rains recorded by Jurassic dunes. *Nature* **2001**, *412*, 64–66. [CrossRef]
19. Scherer, C.M.S.; Goldberg, K. Cyclic cross-bedding in the eolian dunes of the Sergi Formation (Upper Jurassic), Reconcavo Basin: Inferences about the wind regime. *Palaeogeogr. Palaeoclimatol. Palaeoecol.* **2010**, *296*, 103–110. [CrossRef]
20. Brothers, S.C.; Kocurek, G.; Brothers, T.C.; Buynevich, I.V. Stratigraphic architecture resulting from dune interactions: White Sands Dune Field, New Mexico. *Sedimentology* **2017**, *64*, 686–713. [CrossRef]
21. Day, M.; Kocurek, G. Aeolian dune interactions preserved in the ancient rock record. *Sediment. Geol.* **2017**, *358*, 187–196. [CrossRef]
22. Bristow, C.S.; Pugh, J.; Goodall, T. Internal structure of aeolian dunes in Abu Dhabi determined using ground-penetrating radar. *Sedimentology* **1996**, *43*, 995–1003. [CrossRef]
23. Bristow, C.S.; Bailey, S.D.; Lancaster, N. The sedimentary structure of linear sand dunes. *Nature* **2000**, *406*, 56–59. [CrossRef]
24. Bristow, C.S.; Lancaster, N.; Duller, G.A.T. Combining ground penetrating radar surveys and optical dating to determine dune migration in Namibia. *J. Geol. Soc.* **2005**, *162*, 315–322. [CrossRef]
25. Bristow, C.S.; Duller, G.A.T.; Lancaster, N. Age and dynamics of linear dunes in the Namib desert. *Geology* **2007**, *35*, 555–558. [CrossRef]
26. Bristow, C.S. Ground-Penetrating Radar in Dune Sands. In *Ground Penetrating Radar: Theory and Applications*; Jol, H.M., Ed.; Elsevier Science: Amsterdam, The Netherlands, 2009; pp. 273–297.
27. Guillemoteau, J.; Bano, M.; Dujardin, J.-R. Influence of grainsize, shape and compaction on georadar waves; examples of an aeolian dune. *Geophys. J. Int.* **2012**, *190*, 1455–1463. [CrossRef]
28. Girardi, J.D.; Davis, D.M. Parabolic dune reactivation and migration at Napeague, NY, USA: Insights from aerial and GPR imagery. *Geomorphology* **2010**, *114*, 530–541. [CrossRef]
29. Quian, R.; Liu, L. Internal structure of sand dunes in the Badain Jaran Desert revealed by GPR. *IEEE J. Sel. Top. Appl. Earth Obs. Remote Sens.* **2016**, *9*, 159–166. [CrossRef]
30. Phillips, J.D.; Ewing, R.C.; Bowling, R.; Weymer, B.A.; Barrineau, P.; Nittrouer, J.A.; Everett, M.E. Low-angle eolian deposits formed by protodune migration, insights into slipface development at White Sands Dune field, New Mexico. *Aeolian Res.* **2019**, *36*, 9–26. [CrossRef]
31. Elbelrhiti, H.; Andreotti, B.; Claudin, P. Barchan dune corridors: Field characterization and investigation of control parameters. *J. Geophys. Res.* **2008**, *113*, F02S15. [CrossRef]
32. Jol, H.M.; Bristow, C.S. GPR in Sediments:advice on data collection, basic processing and interpretation, a good practice guide. In *Ground Penetrating Radar in Sediments*; Bristow, C.S., Jol, H.M., Eds.; Geological Society London Special Publication: London, UK, 2003; Volume 211, pp. 9–27.
33. Cassidy, N. Ground-Penetrating Radar Data Processing, Modelling and Analysis. In *Ground Penetrating Radar: Theory and Applications*; Jol, H.M., Ed.; Elsevier Science: Amsterdam, The Netherlands, 2009; pp. 141–176.
34. Reynolds, J.M. *An Introduction to Applied and Environmental Geophysics*; Wiley: Hoboken, NJ, USA, 1997; 796p.
35. Parteli, E.J.R.; Duran, O.; Bourke, M.C.; Tsoar, H.; Poschel, T.; Herrmann, H. Origins of barchan dune asymmetry: Insights from numerical simulations. *Aeolian Res.* **2014**, *12*, 121–133. [CrossRef]

36. Bristow, C.S.; Mountney, N. Eolian landscapes: Eolian statigraphy. In *Treatise on Geomorphology*; Shroder, J., Lancaster, N., Eds.; Academic Press: Sand Diego, CA, USA, 2012; p. 11.
37. Cook, R.U.; Warren, A.; Goudie, A.S. *Desert Geomorphology*; UCL Press: London, UK, 1993; 526p.